ARTICLE IN PRESS

Available online at www.sciencedirect.com

SCIENCE DIRECT®

Radiation Physics and Chemistry ▮ (▮▮▮▮) ▮▮▮–▮▮▮

Radiation Physics and Chemistry

www.elsevier.com/locate/radphyschem

Innovative dielectrics for semiconductor technology

R.S. Brusa[a,*], C. Macchi[a,1], S. Mariazzi[a], G.P. Karwasz[a,b], G. Scarel[c], M. Fanciulli[c]

[a]*Dipartimento di Fisica, Università di Trento, Via Sommarive 14, I-38050 Povo, Trento, Italy*
[b]*Facoltà di Ingegneria, Università di Trento, I-38050 Mesiano, Trento, Italy*
[c]*Laboratorio MDM/CNR-INFM, via C. Olivetti 2, 20041 Agrate Brianza, Milano, Italy*

Abstract

The synthesis and the characterization of dielectrics with very high and very low relative permittivity κ, are one of the challenges for scaling the dimensions of microelectronic devices. It will be shown that unique and useful insight on high κ thin films and about the surface termination of internal buried empty space ($\kappa = 1$) can be obtained by combining different positron annihilation spectroscopies. Characterization of nano-cavities in Si and of HfO_2 high κ thin films will be presented and discussed.

Keywords: High κ dielectrics; HfO_2; Buried cavities; Low κ dielectrics; Positron annihilation spectroscopies; Doppler broadening spectroscopy; Doppler broadening spectroscopy in coincidence; Slow positrons

1. Introduction

The *International Technology Roadmap for Semiconductors* (ITRS, 2003) indicates in the year 2010 the achievement of scaling below the 45 nm technology node (the introduction of dynamic random access memories (DRAM) with half metal pitch of 45 nm). The continued scaling of the microelectronic devices is requiring the introduction of new dielectrics materials because the traditional ones have been pushed to their fundamental material limits. There is a strong demand of new dielectrics with either very low or very high permittivity values.

Low κ ($\kappa < 2.6$) dielectrics have to be developed and integrated with low resistivity materials (Cu) to reduce the interconnect delay. Low κ are materials with high porosity that should have good chemical and mechanical properties to survive the integration processes. For achieving high reliability of their integration with Cu, studies of adhesion and contamination must be performed and a very thin low-resistivity barrier, acting as well as efficient "pore shield" must be realized (Maex et al., 2003).

High κ ($\kappa > 10$) dielectrics are required to substitute the dielectric (silicon oxynitride or SiO_2) in the two devices that are the core components of integrated circuits: the capacitor dielectrics used for information storage in the DRAMs and the transistor gate dielectrics used in complementary metal-oxide semiconductor field effect transistors (C-MOSFET) (Kingon et al., 2000). The thickness of presently used dielectric films should be reduced to less than 1 nm to achieve the expected performances, but in these conditions leakage current in the gate would be too high. Therefore, higher κ material is necessary to increase the thickness of the dielectric

*Corresponding author. Fax: +39 0461 881696.
E-mail address: brusa@science.unitn.it (R.S. Brusa).
[1]Permanent address: FIMAT, Facultad de Ciencias Exactas, UNICEN, Pinto 399, B7000GHG Tandil, Argentina.

0969-806X/$ - see front matter © 2006 Elsevier Ltd. All rights reserved.
doi:10.1016/j.radphyschem.2006.03.033

layer while keeping constant the capacitance value. Indeed, in DRAM scaling, the requirement for memory capacitors in smaller cell area can be achieved by decreasing the thickness and/or by increasing the permittivity of the dielectric.

Beyond the introduction of new or improved materials, the traditional scaling can also be overcome with the development of new devices architecture. Among the several emerging new devices (ITRS, 2003) we quote the non-classical Silicon on Insulators (SOI) technologies for C-MOS based on Silicon on Nothing (SON) architectures in which buried empty space is used as insulator for the transistor gate. The empty spaces, which range from submicron to micron size, can be obtained by removing sacrificial layer (Jurczak et al., 2000) or by starting from deep trenches in Si after annealing in hydrogen atmosphere (Mizushima et al., 2000). Another way to produce SOI is also to create cavities of nm and μm size at controlled depth in Si by light ions (He and H) implantation (Cerofolini et al., 2000).

In the following we shall present studies in which positron spectroscopy has been applied for characterizing high κ films and internal surfaces of buried empty spaces in Si. For positron annihilation studies of low κ materials, we refer to some recent reviews and papers (Brusa et al., 2004, 2005a; Petkov et al., 2003; Gidley et al., 2001; Dull et al., 2001), and to the lectures presented in this workshop.

2. Positron measurements and analysis

Positron measurements were carried out with a slow positron beam (Zecca et al., 1998) coupled to a sample chamber equipped with two high purity germanium detectors (HPGe) 45% efficiency, 1.4 keV resolutions at 511 keV, in a 180° configuration. Two types of positron spectroscopy were used: (1) depth profiling with Doppler Broadening Spectroscopy (DBS) to study the low momentum region around the 511 keV peak position due to positron annihilation with valence electrons; (2) DBS in coincidence (C-DBS) to study the high momentum region of the 511 keV annihilation line, for extracting element-specific information on the atoms around the annihilation site (Krause-Rehberg and Leipner, 1999).

In the DBS measurements, the 511 keV annihilation peak was measured as a function of the positron implantation energy E. The mean positron implantation depth $\bar{z}$ is calculated as $\bar{z} = (40/\rho)E^{1.6}$, with $\bar{z}$ in nm when the density ρ and E are expressed in g/cm^3 and keV, respectively.

The annihilation peak was characterized by the normalized shape parameter S_n ($S_n = S_{measured}/S_{bulk-Si}$). The parameter S was calculated as the ratio of the counts in the central area of the peak ($|511-E_\gamma| \leqslant 0.85$ keV) to the total area of the peak ($|511-E_\gamma| \leqslant 4.25$ keV), with E_γ the Doppler shift in energy of the annihilation γ-ray.

$S_n(E)$ is a linear combination of the characteristic S values multiplied by the fraction f of positron annihilating at the surface [S_S;$f_S(E)$], in the Si bulk [S_b;$f_b(E)$] and in the different j state [S_j;$f_j(E)$]:

$$S_n(E) = S_S f_S(E) + \sum_j S_j f_j(E) + S_b f_b(E), \quad (1)$$

$$f_S(E) + \sum_j f_j(E) + f_b(E) = 1 \quad \forall E. \quad (2)$$

The j states can be trap sites, film/substrate interface, and different film layers. At selected implantation energy E the C-DBS curve $C(E, E_\gamma)$ was measured. A reference coincidence annihilation line $C_b(E_\gamma)$ is measured in the bulk of the reference material. Ratio curves were constructed with the aid of this reference curve (Asoka-Kumar et al., 1996). Each curve $C(E, E_\gamma)$ is a linear combination of different terms:

$$C(E, E_\gamma) = C_S(E_\gamma) f_S(E) + \sum_j C_j(E_\gamma) f_j(E) + C_b(E_\gamma) f_b(E), \quad (3)$$

where $C_S(E_\gamma)$ and $C_j(E_\gamma)$ are the characteristic annihilation line of positron annihilating at the sample surface and in state j, respectively.

The physical information on the state j (open volume defects, their decoration, morphological change of the structure), are contained in the characteristic S_j values and in the shape of the $C_j(E_\gamma)/C_b(E_\gamma)$ ratio curves (Asoka-Kumar et al., 1996; Brusa et al., 2002).

The characteristic S_j values are found by fitting the S_n vs. E DBS curves with the stationary positron diffusion equation model (van Veen et al., 1990; Dupasquier and Ottaviani, 1995; Brusa et al., 2000). The $f_j(E)$ curve can be obtained directly from the diffusion model (Dupasquier and Ottaviani, 1995; Brusa et al., 2000). In specific cases, knowing $f_j(E)$, $f_S(E)$, $f_b(E)$ and having $j+1$ measured $C(E, E_\gamma)$ profiles, the $C_j(E_\gamma)/C_b(E_\gamma)$ and $C_S(E_\gamma)/C_b(E_\gamma)$ curves can be obtained by constructing with Eq. (3) a system of $j+1$ equations (Brusa et al., 2005a, b).

We found the model presented by Dupasquier and Ottaviani (1995), suited for the analysis of homogenous samples in which distributions of open volume defects are present (Section 3). The model by van Veen et al. (1990) was applied to study multilayer systems (Section 4).

3. Empty spaces in Si ($\kappa = 1$)

The internal surfaces of the cavities (empty spaces), produced as described in the introduction, can be purposely decorated or can become decorated by

undesired impurities during the technological processes. In order to explore the potential of positrons probe the state of internal surfaces we have studied *p*-type (1 0 0) Si samples, Czochralski-grown (1.7–2.5 Ω cm), implanted with He^+ ions at 20 keV (dose of 2×10^{16} ions/cm^2). Samples were annealed in vacuum for 2 h at 900 °C. Annealing at this high temperature produces agglomeration of He (formation of bubbles) and then their complete out-diffusion (Brusa et al., 2000; Cerofolini et al., 2000.). At the end of the process, empty cavities are left in the Si crystal. TEM (Transmission Electron Microscopy) analysis reveals a layer of nano-cavities centred around 200 nm in the sample implanted by He. The TEM analysis however could not clarify whether the internal surfaces of the cavities were clean or decorated by impurities.

In Fig. 1, the obtained S_n vs. E curve for the sample implanted with He is reported. The curve was fitted with two defect profiles centred, respectively, at 23 and 193 nm. The second profile is due to defects leading to $S=1.112$, and clearly corresponds to the distribution of nano-cavities seen by TEM. The first one ($S=0.91$) corresponds to smaller defects. In the inset of Fig. 1, the f fractions extracted by the fitting procedure of positron annihilating at the Si surface, into the two defect types (f_d and f_c), and in silicon bulk are reported. The characteristic ratio curves were obtained by solving the system of equations (Eq. (3)) with the f fractions and the ratio curve measured at four positron implantation energies (0.15, 0.35, 6, 18 keV). The ratio curve as measured at 6 keV and the characteristic ratio curves for the defects, the cavities and the surface are shown in Fig. 2.

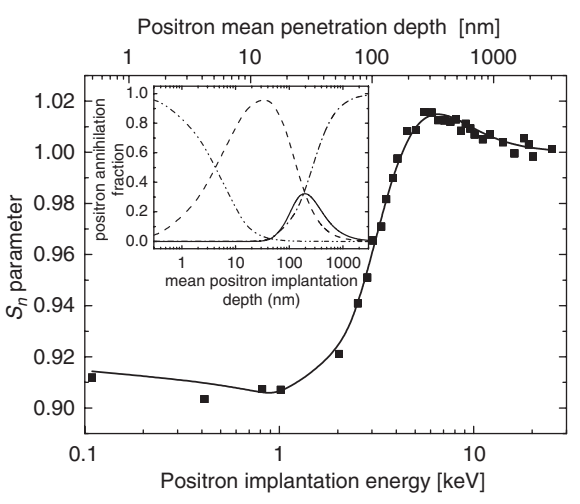

Fig. 1. S_n versus positron implantation energy and positron mean implantation depth (upper axis). The continuous line is the best fit with the diffusion model (Brusa et al., 2000). In the inset the positron annihilation probability: f_S at the surface (dash–dot–dot); f_d in the surface defects (dash); f_c in the cavities (continuous line); f_b in the bulk (dash–dot).

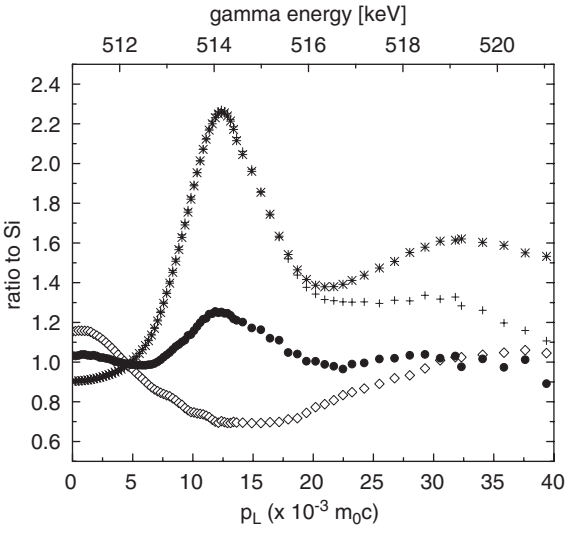

Fig. 2. Ratio curves to bulk Si. Full dots, ratio of the annihilation peak as measured at 6 keV. Extracted characteristic ratio curve for surface defects (crosses), silicon dioxide at the surface (stars), cavities (open diamond). p_L is the longitudinal momentum of the positron–electron pair.

From Fig. 2 it appears that the shape of the characteristic ratio curve for the deeper defect is typical for positron annihilation in "clean" cavities (Brusa et al., 2005b). The shape of the curve related to the superficial defects indicates annihilation in oxygen complexes (Brusa et al., 2001) because of the peak superimposed to the characteristic ratio curve of annihilation at the surface native oxide, for $E_\gamma<516$ keV. In this sample, lifetime spectra obtained with a pulsed positron beam (Bauer-Kugelmann et al., 2001), were de-convoluted with two lifetimes: the first one around 500 ps typical of annihilation at the walls of large cavities and the second one due to annihilation in the bulk (225 ps). Only around 3 keV the second lifetime increases by 15–20 ps, from which we conclude that the decorated surface defects have a lifetime not too much different from the Si bulk lifetime.

A similar analysis was also performed on He–H co-implanted sample (Brusa et al., 2006). In that case it was observed that, beyond clean cavities, in contrast there are internal surfaces below blisters (revealed by TEM) that are oxygen decorated.

4. High-κ: hafnium oxide thin films

4.1. Samples and characterization

Hafnium oxide films were grown by Atomic Layer Deposition (ALD) in a flow type ASM-Microchemistry F-120 reactor, alternating pulses of $HfCl_4$ and H_2O. The

films were deposited on *p*-type Si (100) wafers without removing the native SiO_2 (1.2 nm thick). The $HfCl_4$ and H_2O sources were kept at 160 and 18 °C, respectively, during deposition. The $HfCl_4$ and H_2O precursors were injected in the growth chamber by N_2 in 4 and 6 s long pulses, respectively. The films were grown at 200 °C with 190 pulse/purge cycles. During growth, the pressure in the reactor was of the order of 10^{-3} bar. These conditions resulted in films 29 nm thickness. Post-deposition thermal annealing (TA) was performed in vacuum (10^{-8} Torr) for 10 min at 900 °C, and in O_2 ambient (10^{-1} Torr) for 6 min at 800 °C.

By time-of-flight-secondary ion mass spectrometry (TOF-SIMS), the main contaminants in the as-grown film were found to be chlorine and carbon (Scarel et al. 2003). While Cl was homogenously distributed through the film (about 8% of the amount of O), C was found mainly concentrated at the interface with the substrate. The Cl content was found to decrease after TA in a N_2 atmosphere and the films were found to transform from an amorphous to a polycrystalline structure (Scarel et al., 2004a). The permittivity of the as-grown film is about one half of the value expected for bulk HfO_2 ($\kappa = 22$) and is further reduced by the TA.

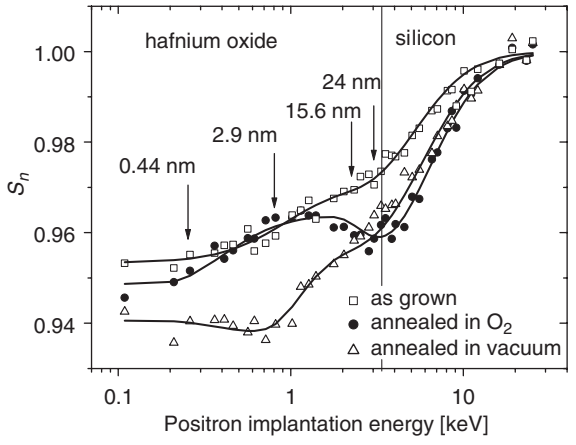

Fig. 3. S_n versus positron implantation energy for hafnium oxide films: as-grown, annealed in vacuum and annealed in O_2. The continuous lines are best fit with VEPFIT (van Veen et al., 1990).

4.2. Positron results and discussion

In Fig. 3 the S_n vs. E DBS measurements for the three samples (as grown film, and those annealed in vacuum and in oxygen) are shown. The best fits were obtained by the VEPFIT program, and the main parameters of the fit are reported in Table 1. The as-grown film was fitted with two layers: the film and the Si substrate. The two applied TA produce different film modifications: the S_n values of the films decrease in both cases, but this reduction is more pronounced in the vacuum annealed film, pointing to a decrease of open volume defects. Moreover, the sample annealed in O_2 presents a thin interface layer, while the sample annealed in vacuum shows a thin surface layer. Both layers have a low S_n value, indicating presence of O or contaminants (C, Cl).

The film ratio curves to Hf reference curve (C-DBS measurements) are presented in Fig. 4. At present we are not able to extract the film characteristic curves due to the lack of the characteristic curves of the contaminants and of O, and we can make only qualitative statements comparing the film ratio curves with those of SiO_2 and Si. Interesting insights are nevertheless obtained. At 0.25, 0.8 and 2.3 keV practically all positrons annihilate in the film (93% at 2.3 keV) and the curves do not need to be corrected for the presence of the substrate. At 3.0 keV the positron fractions annihilating into the Si substrate becomes important (< 30%) and the film ratio curves are expected to be higher in the 513–530 keV range by a few percent. The subtraction of the Si contribution would also require a careful evaluation of positron diffusion to the Si/film interface.

In hafnia (HfO_2), positrons may be sensitive to neutral oxygen vacancies, hafnium vacancies and oxygen defects; oxygen defects in hafnia are negatively charged (Foster et al., 2002a). In the case of positron annihilation in neutral O vacancies, an increased signal

Table 1
Main parameters obtained by fitting the S_n vs. E curves of Fig. 3 with VEPFIT program. L_+ denotes the positron diffusion length, d_I, d_{II}, d_{III} the thickness of the layers

	29 nm Hf–O on Si (9.7 g/cm^3)									Si
	Layer I			Layer II			Layer III			
	S_n	L_+ (nm)	d_I (nm)	S_n	L_+ (nm)	d_{II} (nm)	S_n	L_+ (nm)	d_{III} (nm)	L_+ (nm)
As-grown				0.970	4	29				250
Annealed O_2				0.964	1	25 ± 1	0.94	1.5 ± 0.5	4 ± 1	250
Annealed vacuum	0.936	1	6 ± 1	0.958	1	24				250

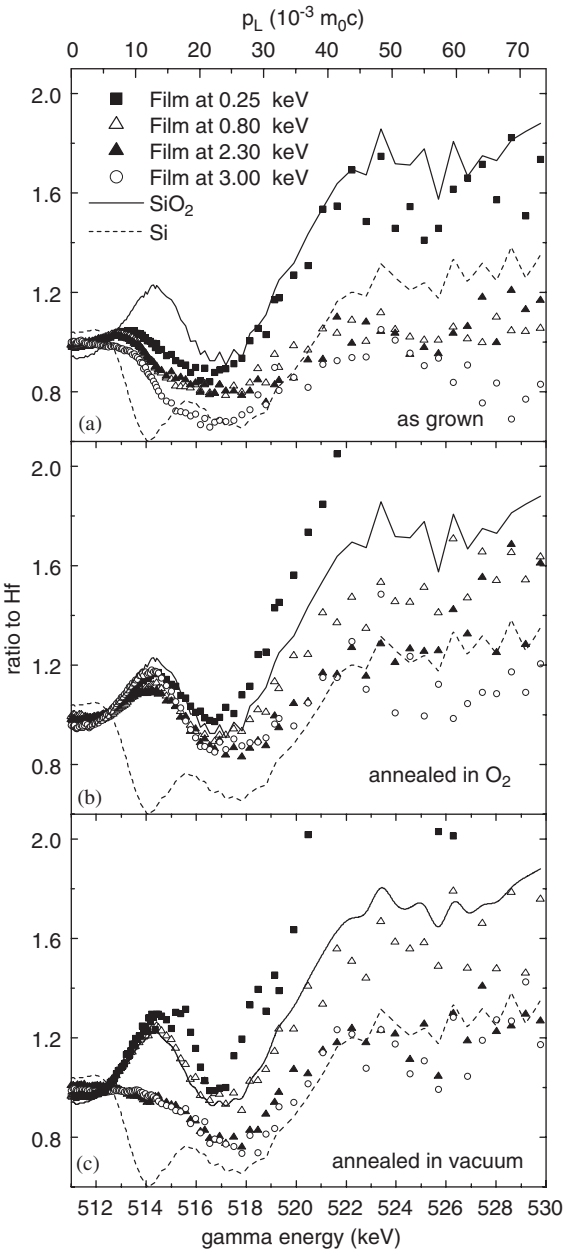

Fig. 4. Ratio curves to bulk Hf. Ratio of the annihilation peak as measured at 0.25, 0.8, 2.3 and 3.0 keV positron implantation energies. The ratio curves for SiO_2 and Si are also presented. (a) As grown film; (b) film annealed in O_2; (c) film annealed in vacuum.

from Hf (annihilation with 5*d* electrons) would be expected in the ratio curves. In stoichiometric hafnia we would expect that positron are more localized around O atoms, due to the ionic character of this solid.

As-grown film (Fig. 4a): the sample surface is slightly rich in O, while the film is homogeneous and positrons annihilate mainly with Hf with no, or small contribution from oxygen (no oxygen peak around 514 keV). This finding points to a disordered structure with O vacant sites. The low curve at 3 keV, starting from 515 keV, seems also to be affected by the contaminants (C or/and Cl) at the interface with silicon.

Film annealed in O_2 (Fig. 4b): in this case there is a strong variation of the surface in comparison with the as-grown film, and the film bulk appears rich in O (first peak around 514.5 keV) with a ratio curve that is very similar in shape to that of SiO_2. This behaviour is in agreement with the fact that annealing in O is expected to produce O diffusion inside the film (Foster et al., 2002b). Here it is difficult to say whether if the film has become stoichiometric or if it is rich of O interstitial negative defects after annealing. To have an answer, this curve should be compared with a stoichiometric hafnia sample (work in progress).

Film annealed in vacuum (Fig. 4c): the film up to few nanometers below the surface is richer in oxygen than the as-grown film. Also here ratio curve of the film resembles SiO_2. In this case the bulk of the film, up to the interface, is more homogeneous than in the as grown one, but again positrons annihilate mainly with Hf atoms. This result indicates that vacuum annealing leaves a more ordered film (lower S_n value) but still with oxygen vacancies.

The possible formation of SiO_2 at the surface of the TA samples can be explained by the diffusion of Si towards the surface as shown by Ferrari and Scarel (2004) in very thin films (10 nm).

5. Conclusion

We have shown as the positron probe is well suited (a) for giving information on the internal termination of buried cavities in Si (b) for characterizing variations in the defect distribution (O vacancies, interstitial O) of thin high κ films after TA in different ambients.

Acknowledgements

This work was partially supported by the Ministero dell' università e della Ricerca Scientifica e Tecnologica (MURST).

References

Asoka-Kumar, P., Alatalo, M., Ghosh, V.J., Kruseman, A.C., Nielsen, B., Lynn, K.G., 1996. Increased elemental specificity of positron annihilation spectra. Phys. Rev. Lett. 77, 2097–2100.

Bauer-Kugelmann, W., Sperr, P., Kögel, G., Triftshäuser, W., 2001. Latest version of the Munich pulsed low energy positron system. Mater. Sci. Forum 363–365, 529–531.

Brusa, R.S., Karwasz, G.P., Tiengo, N., Zecca, A., Corni, F., Tonini, R., Ottaviani, G., 2000. Formation of vacancy cluster and cavities in He-implanted silicon studied by slow-positron annihilation spectroscopy. Phys. Rev. B 61 (15), 10154–10166.

Brusa, R.S., Deng, W., Karwasz, G.P., Zecca, A., Pliszka, D., 2001. Positron annihilation study of vacancy-like defects related to oxygen precipitates in Czochralski-type Si. Appl. Phys. Lett. 79, 1492–1494.

Brusa, R.S., Deng, W., Karwas, G.P., Zecca, A., 2002. Doppler-broadening measurements of positron annihilation with high-momentum electrons in pure elements. Nucl. Instrum. Methods B 194, 519–531.

Brusa, R.S., Spagolla, M., Karwasz, G.P., Zecca, A., Ottaviani, G., Corni, F., Bacchetta, M., Carollo, E., 2004. Porosity in low dielectric constant SiCOH films depth profiled by positron annihilation spectroscopy. J. Appl. Phys. 95 (5), 2348–2354.

Brusa, R.S., Macchi, C., Mariazzi, S., Karwasz, G.P., 2005a. Porosity of low κ materials studied by slow positron beams. Acta Phys. Pol. A 107 (4), 702–711.

Brusa, R.S., Macchi, C., Mariazzi, S., Karwasz, G.P., Egger, W., Sperr, P., Kögel, G., 2005b. Absence of positronium formation in clean buried nanocavities in *p*-type silicon. Phys. Rev. B 71 (245320), 1–5.

Brusa, R.S., Macchi, C., Mariazzi, S., Karwasz, G.P., Egger, W., Sperr, P., Kögel, G., 2006. Decoration of buried surfaces in Si detected by Positron Annihilation Spectroscopy. Appl. Phys. Lett. 88, 011920-1, 011920-3.

Cerofolini, C.F., Corni, F., Frabboni, S., Nobili, C., Ottaviani, G., Tonini, R., 2000. Hydrogen and helium bubbles in silicon. Mater. Sci. Eng. R 27, 1–52.

Dull, T.L., Frieze, W.E., Gidley, D.W., Sun, J.N., Yee, A.F., 2001. Determination of pore size in mesoporous thin films from the annihilation lifetime of positrons. J. Phys. Chem. B 105, 4657–4662.

Dupasquier, A., Ottaviani, G., 1995. Defect profiling by positron beams and other techniques. In: Dupasquier, A., Mills, Jr., A.P. (Eds.), Positron Spectroscopy of Solids. North-Holland, Amsterdam, pp. 581–657.

Ferrari, S., Scarel, G., 2004. Oxygen diffusion in atomic layer deposition deposited ZrO_2 and HfO_2 thin films on Si (1 0 0). J. Appl. Phys. 96 (1), 144–149.

Foster, A.S., Lopez, G., Shluger, A.L., Nieminen, R.M., 2002a. Vacancy and interstitial defects in hafnia. Phys. Rev. B 65 (174117), 1–13.

Foster, A.S., Shluger, A.L., Nieminen, R.M., 2002b. Mechanism of interstitial oxygen diffusion in hafnia. Phys. Rev. Lett. 89(22), 225901, 1–4.

Gidley, D.W., Lynn, K.G., Petkov, M.P., Weber, M.H., Sun, J.N., Yee, A.F., 2001. Depth-profiled positron annihilation spectroscopy of thin insulation films. In: Surko, C.M., Gianturco, F.A. (Eds.), New Directions in Antimatter Chemistry and Physics. Kluwer Academic Publishers, Dordrecht, pp. 151–171.

ITRS, 2003. Semiconductor Industry Association, International Technology Roadmap for Semiconductors ed., 2003 http://www.public.itrs.net/Files/2003ITRS/Home2003.htm

Jurczak, M., Skotnicki, T., Paoli, M., Tomen, B., Martins, J., Regolini, J.L., Dutartre, D., Ribot, P., Lenoble, D., Pantel, R., Monfray, S., 2000. Silicon-on-Nothing (SON)-an innovative process for advances CMOS. IEEE Trans. Electron. Dev. 47 (11), 2179–2187.

Kingon, A.I., Maria, J.-P., Steiffer, S.K., 2000. Alternative dielectrics to silicon dioxide for memory and logic devices. Nature 406, 1032–1038.

Krause-Rehberg, R., Leipner, H.S., 1999. Positron Annihilation in Semiconductors, Defect Studies, Springer series in Solid State Science. Springer, Berlin, Heidelberg.

Maex, K., Baklanov, M.R., Shamiryan, D., Iacopi, F., Brongersma, S.H., Yanovitskaya, Z.S.J., 2003. Low dielectric constant materials for microelectronics. Appl. Phys. 93, 8793–8841.

Mizushima, I., Sato, T., Taniguchi, S., Tsunashima, Y., 2000. Empty-space in-silicon technique for fabricating a silicon-on-nothing structure. Appl. Phys. Lett. 77, 3290–3292.

Petkov, M.P., Wang, C.L., Weber, M.H., Lynn, K.G., Rodbell, K.P., 2003. Positron annihilation techniques suited for porosity characterization of thin films. J. Phys. Chem. B 107, 2725–2734.

Scarel, G., Wiemer, C., Ferrari, S., Tallarida, G., Fanciulli, M., 2003. Effects of growth temperature on the properties of HfO_2 films grown by atomic layer deposition. Proc. Estonian Acad. Sci. Phys. Math. 52 (3), 308–320.

Scarel, G., Spiga, S., Wiemer, C., Tallarida, G., Ferrari, S., Fanciulli, M., 2004a. Trends of structural and electrical properties in atomic layer depositited HfO_2 films. Mater. Sci. Eng. B 109, 11–16.

van Veen, A., Schut, H., de Vries, J., Hakvoort, R.A., Ijpma, M.R., 1990. VEPFIT program. In: Schultz, P.J., Massoumi, G.R., Simpson, P.J. (Eds.), AIP Conf. Proc. 218, Positron Beams for Solids and Surfaces, London, Ontario, 1990, pp. 171–196.

Zecca, A., Bettonte, M., Paridaens, J., Karwasz, G.K., Brusa, R.S., 1998. A new electrostatic positron beam for surface studies. Meas. Sci. Technol. 9, 409–416.